

Research papers

Analysis of the timing of phase changes in the chlorophyll concentration in the East/Japan Sea



Young-Heon Jo ^a, Hyun-Cheol Kim ^{b,*}, Seunghyun Son ^{c,d}, Dohoon Kim ^e

^a Department of Oceanography, Pusan, National University, Busan 46241, Republic of Korea

^b Department of Polar Remote Sensing, Korea Polar Research Institute, Incheon 21990, Republic of Korea

^c NOAA/NESDIS Center for Satellite Application and Research, Colledge Park, MD 20740, USA

^d CIRA, Colorado State University, CO 80523, USA CIRA, Colorado State University, CO 80523, USA

^e Department of Marine & Fisheries Business and Economics, Pukyong National University, Busan 48513, Republic of Korea

ARTICLE INFO

Article history:

Received 16 November 2015

Received in revised form

14 July 2016

Accepted 12 August 2016

Available online 12 August 2016

ABSTRACT

Geographically heterogeneous linear and non-linear chlorophyll-a (CHL) trends in the East Sea/Japan Sea (EJS) region were analyzed based on monthly mean Moderate Resolution Imaging Spectroradiometer (MODIS) CHL data from January 2003 to December 2012. The non-linear trends were derived from the residuals of decomposed CHL time series using ensemble empirical mode decomposition (EEMD). To understand the general spatial and temporal variability of the non-linear CHL trends, a complex empirical orthogonal function (CEOF) was employed. The first two CEOF modes indicate that an upward CHL trend occurred in 2007 with 95.6% variance, whereas a downward CHL trend occurred in 2009 with 4.1% variance. Furthermore, the specific timing of the phase changes in CHL was calculated based on upward or downward non-linear trends of CHL for six major regions of interests.

To examine the dominant forces in phase changes in CHL, the Multivariate El Niño-Southern Oscillation (ENSO) Index (MEI) was used. We determined that the local turning patterns of CHL over the last ten years were closely related to changes in ENSO events, which were also associated with changes in the total amount of fish catches off the east coast of the Korean Peninsula. These results also suggest that the short-term total amount of fish catches may be predictable based on the remotely sensed non-linear CHL observations.

© 2016 Elsevier Ltd. All rights reserved.

1. Introduction

The East Sea/Japan Sea (EJS) is a marginal sea located in the northwestern Pacific and is surrounded by Korea, Japan, and Russia (Fig. 1). The EJS is connected to adjacent seas by five shallow straits. There are four surface current systems in the EJS: the Tsushima Warm Current (TWC), the East Korean Warm Current (EKWC), the North Korean Cold Current (NKCC), and the Liman Current. The NKCC and the EKWC meet along the east coast of Korea. The warm saline water of the TWC passes through the Korean Strait, where the flow often bifurcates into western and eastern branches. The EKWC later turns eastward between 37°N and 39°N, where it meets the NKCC (Seung and Kim, 1989) and becomes a sub-polar front (SF). The NKCC originates from the Liman Current coming from the Tatar Strait, and some of the denser water in the NKCC intrudes along the coast below the surface.

Two blooms, appearing in the spring and fall, are typical feature

of phytoplankton variability in the temperate zone. The spatial distributions of phytoplankton blooms are specific features of the EJS. Blooms of phytoplankton (chlorophyll-a (CHL)) increasing) appear in the spring (Yamada et al., 2004; Yoo and Kim, 2004; Kim et al., 2007) and fall in the EJS (Yamada et al., 2004; Kim et al., 2007). Ocean color data for 1997–2002 show the inter-annual variability of CHL in the EJS; earlier spring blooms occur during El Niño years, and later spring blooms occur during La Niña years due to the associated wind patterns (Yamada et al., 2004). In particular, the spring bloom duration of 1999 in the EJS was influenced by La Niña through wind stress changes (Yoo and Kim, 2004). The winds play an important role in the seasonal variability of CHL; a spring bloom began approximately 10 days after the wind stress weakened, and a fall bloom started approximately a week after the wind strengthened (Kim et al., 2007).

Several studies have found that the impacts of climatic regime shifts within the EJS are significant with respect to the marine ecosystem and fishery resources. Zhang et al. (2004) reported that the total biomass in the EJS ecosystem increased by 15% and the total catch production increased by 48% due to the 1976 regime shift. Similarly, Zhang et al., (2007) analyzed the before and after

* Corresponding author.

E-mail address: kimhc@kopri.re.kr (H.-C. Kim).

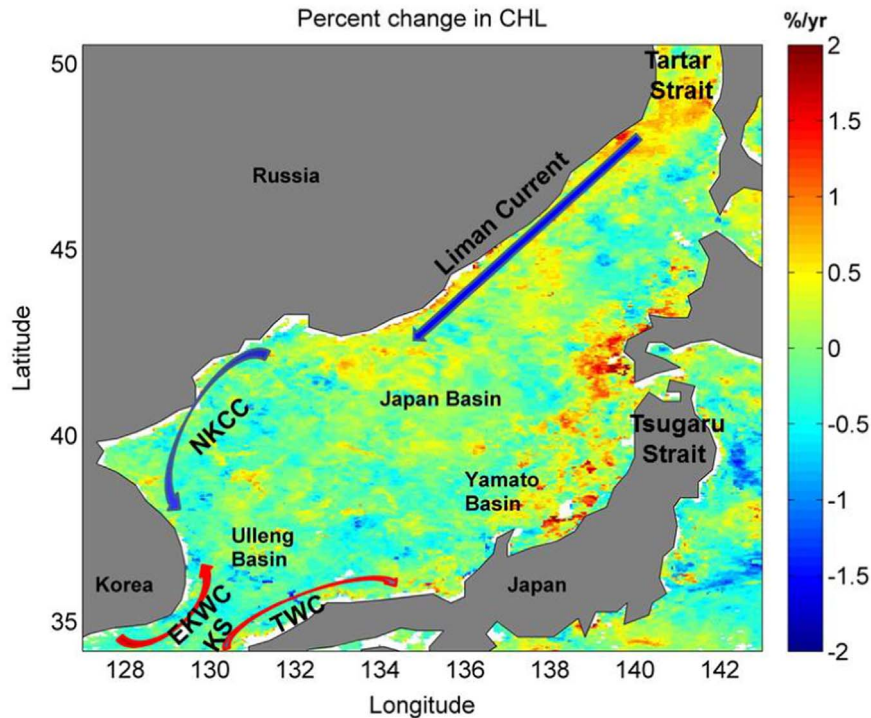


Fig. 1. Percent changes in CHL from January 2003 to December 2012. Major sea surface currents are illustrated. TWC stands for the Tsushima Warm Current, EKWC stands for the East Korean Warm Current (EKWC), and NKCC stands for the North Korean Cold Current.

effects of the 1988/89 regime shift on the structure and function of the southwestern EJS ecosystem and reported that the total biomass of all species groups in the ecosystem increased by 59% after the 1988/89 regime shift. Recently, Tian et al. (2013) reported that the abundance trends of squid were largely forced by environmental factors with latitudinal differences in the response to the climatic regime shift. Seasonal and inter-annual CHL variability associated with climatic regime shifts has been reported. Such changes can result in significant changes in latitudinal fishery resources within the EJS (Zhang et al., 2000).

Studies have reported that there are indications of climate change in Korean waters. For instance, Kim and Yoo (1996) reported evidence that temperatures increased in the mid-1970s, and fishery resources reflected these changes. There were significant increases in the biomass of zooplankton within the last two decades in the Yellow Sea (Son et al., 2005), in the East/Japan Sea (Zhang et al., 2000), and along the southern coast of Korea (Kim and Kang, 2000). It has been shown that the variability of fishery biomass corresponded to climate change during the last several decades around the Korean Seas. The 1976 regime shift in the North Pacific caused a decrease in the biomass of sauries, an increase in the biomass of sardines in the Korea Seas (Zhang et al., 2000), and an increase in the total catch of anchovies and mackerels along the southern coast of Korea (Kim and Kang, 2000). The study showed that there are high correlations between environmental variations derived from water transparency (Secchi depth) and CHL in Korean waters.

To understand CHL variability due to climate change, long-term CHL observations are necessary. Because we do not have enough CHL observations to resolve a regime shift resulting from global climate change, we analyzed the timing of phase changes (either downward or upward trends) in CHL to detect and understand when CHL changed significantly. The timing of phase changes in CHL is not comparable to a regime shift, but it shows the short-term variability in the middle of a regime shift. Understanding phase changes in CHL is important because it relates ecological

processes of climatological forces to the prediction fishery resources (e.g., Bertolo et al., 1999; Polovina et al., 2001; Platt et al., 2003). Platt et al. (2003) reported that the survival of larval fish depends on the timing of the local spring bloom of phytoplankton based on remote-sensing satellite data and a long-term data set of haddock recruitment off the eastern continental shelf of Nova Scotia, Canada.

Thus, in this study, we addressed how CHL has changed in the last ten years based on linear and non-linear trends. The conventional linear trend shows only steady, straight-line increases or decreases, with the trend line going up or down. In contrast, a non-linear trend shows the local maximum or minimum in a time series, enabling us to determine the timing of a turning point. The non-linear trend of CHL derived from the residual of ensemble empirical mode decomposition has a local maximum or local minimum, which we can further analyze for general spatial and temporal patterns based on complex empirical orthogonal functions (Section 3.1), the specific timing of turning points (Section 3.2), and the relationship between non-linear CHL patterns and fishery resources (Section 3.3). These three analyses are the main objectives of this study.

2. Data and methods

MODIS Ocean Color, Sea Surface Temperature, Multivariate El Niño-Southern Oscillation (ENSO) Index, and Total Fish Catches: Moderate Resolution Imaging Spectroradiometer (MODIS) reprocessed 2013 data were used in this study. Monthly Standard Mapped Image (SMI) CHL using the Ocean Color Chlorophyll version 3 (OC3) algorithm from January 2003 to December 2012 for MODIS was obtained from the NASA ocean biology processing group (<http://oceancolor.gsfc.nasa.gov>). The spatial resolution of the MODIS data is 4×4 km. The monthly data were divided into a subset for the EJS. To examine the dominant forces on CHL, the monthly mean Multivariate El Niño-Southern Oscillation (ENSO)

Index (MEI) (<http://www.esrl.noaa.gov/psd/enso/mei/>) was used.

Fishery catch data were obtained from the Korean Fishery Information Service (www.fips.go.kr). To calculate the total amount of catches in the EJS region, the catch amount of coastal and offshore fisheries by species, cities, and provinces within the EJS region were aggregated. The use of fishery catch data from commercial marine fisheries (coastal and offshore fisheries) has limitations in terms of analyzing the range of the distribution areas for fish species because it is biased by operational and social factors of fishing that are difficult to quantify and filter. Because the data on the total biomass of fish stocks were also not available, we used data for the total amount of catches of coastal and offshore fish from 2003 to 2012 off the east coast of the EJS.

2.1. Complex empirical orthogonal function

The Complex (time domain) Empirical Orthogonal Function was introduced to analyze a set of time series data that has a phase lag by adding components that are the original time series data rotated by 90 degrees on a complex plane using a Hilbert transform (Von Storch and Zwiers, 1999). The benefit of using CEOF is that we can analyze not only spatial and temporal amplitudes but also changes in spatial and temporal phases (Merrifield and Guza, 1990). The phase changes are shown in Fig. 6b and d. Accordingly, the CEOF is an alternative method for detecting propagating signals, and decomposed CEOF modes reveal spatial structures that propagate in space and vary in time.

$$CHL(x, y, t) = \sum_{m=1}^{tn} PC_m(t)S_m(x, y) \quad (1)$$

$$PC_m(t) = A_m(t)\exp[i\phi_n(t)],$$

$$S_m(x, y) = B_m(x, y)\exp[i\phi_n(x, y)]. \quad (2)$$

PC_m and S_m represent temporal and spatial functions of CHL, respectively. Whereas the PC_m reveals the dominant time-based patterns, such as semi-annual, annual, inter-annual, decadal, etc., S_m reveals the highest and the lowest changes in the mode in response to the each temporal EOF mode. Thus, the PC_m and S_m allow us to identify the dominant patterns of temporal and spatial signals in the long-term time series measurements according to the variance. tn is 120 months for this study. x and y are zonal and meridional locations of each grid point for CHL measurements. A_m and B_m are the amplitudes of temporal and spatial EOFs, respectively. ϕ_n is the phase for temporal and spatial EOFs. EOF has been well accepted as a tool to analyze the critical temporal and spatial changes of dominant features in response to different variances. In this study, we employed CEOF to analyze non-linear trends and determine the local phase changes from the temporal CEOF based on $PC_m(t)$ and those associated with the spatial CEOF. Thus, this study focuses not only on dominant phase and amplitude changes based on the CEOF but also on local temporal and spatial changes using Ensemble Empirical Mode Decomposition (EEMD).

2.2. Ensemble empirical mode decomposition

Huang et al. (1998) demonstrated the differences between Fourier Analysis, Wavelet analysis and Hilbert Spectral Analysis (HAS). Empirical Mode Decomposition (EMD) of HAS is an empirical technique for analyzing non-stationary and non-linear time series (Huang et al., 1998). Based on EMD, the data are initially decomposed into a set of Intrinsic Mode Function (IMF) components. According to Huang et al. (1998), an IMF represents a simple oscillatory mode and in general has variable amplitude and frequency expressed as functions of time. One of the major problems

with conventional EMD is the frequent appearance of mode mixing, which can produce signals of disparate scales residing in the same IMF component. To overcome this problem, Wu and Huang (2009) introduced a newer version of EMD called Ensemble Empirical Mode Decomposition (EEMD), which produces improved IMF components calculated as the mean of an ensemble of trials, each consisting of the signal plus white noise of finite amplitude. Because the IMF components are essentially independent and can thus be linearly combined, we can reconstruct the residual $R(t)$ from the original record, $CHL(t)$, and summation of all IMFs,

$$R(t) = CHL(t) - \sum_{m=1}^n IMF_m, \quad (3)$$

where n represents the total number of IMFs, which can be determined by 'log(total number of data points)-1' (Wu and Huang, 2009; Wu and Huang, 2005). According to Huang and Wu (2008), the IMF components are often physically meaningful, so they can provide insight into the processes involved. The non-linear trends of CHL were obtained from Eq. (3). The non-linear trend is also called the adaptive trend according to Huang et al. (1998) because the filtering processes to determine IMFs are based on the data adaptive method. The benefit of using EEMD is that we can obtain two components in the CHL observations: oscillatory components and a trend. Unlike Fourier Transform, EEMD is a data adaptive method where each decomposed mode is determined objectively.

The advantage to using HHT is to estimate the instantaneous frequency, enabling us to understand the phase changes (θ) of dynamical signals with time. The instantaneous frequency (ω) is defined as follows:

$$\omega(t) = \frac{d\theta(t)}{dt}. \quad (4)$$

Once the instantaneous frequency (as a function of time) of a time series has been generated, the time-dependent spectrum can be determined. Using Eq. (4), the timing of each turning point was determined to analyze the propagation of regional CHL changes and to identify the phase changes in CHL.

2.3. Cumulative Sums

The Cumulative Sums method is applied to the MEI to examine the impact of ENSO events on the changing phase of CHL. The method of cumulative sums is usually used to detect points that may correspond to abrupt changes, such as regime shifts. Cumulative sums (CUSUMs) represent the running total of the deviations of the first n observations from a mean based on the same interval (Page, 1954; Wetherill and Brown, 1991; Hawkins and Olwell, 1998; Breaker, 2007). The Cumulative Sums (CS) can be expressed as follows:

$$CS = \sum_{t=1}^n (x_t - \bar{x}) \quad (5)$$

where x_t represents the n th observation, \bar{x} is the mean of x_t from $t=1$ to n , and CS is plotted versus time to produce the so-called CUSUM chart. Abrupt changes in the slope of the CUSUM often reflect change points. The benefit of using Cumulative Sum is that we can recognize the timing of sudden changes in observation time series. This method is particularly sensitive to change points, such as regime shifts in coastal observations of SST (Breaker, 2007; Jo et al., 2014). Abrupt changes in the slope of the CUSUM often reflect change points which, in our case, could indicate a regime shift. The coastal temperature may increase or decrease, depending on the locations as a result of the regime change. These events have time scales on the order of six months and may have a long-term impact on the mean state of the ocean.

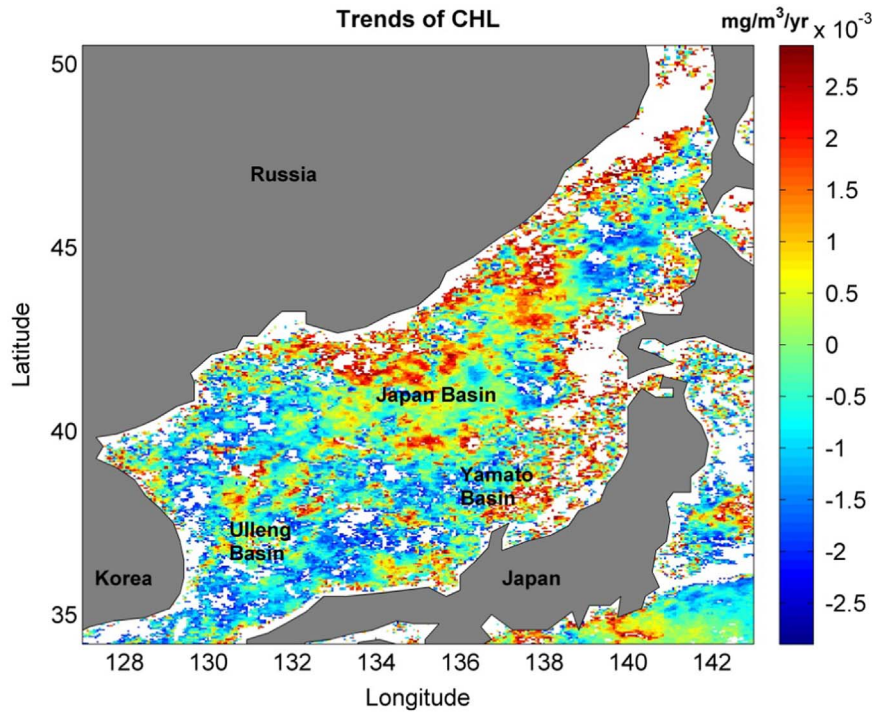


Fig. 2. Linear trends in CHL over ten years from January 2003 to December 2012 ($p=0.05$). CHL trends below 95% significance level were masked out, as shown with white.

3. Results

3.1. Regional linear and non-linear trends of CHL

To understand the variability of CHL in the EJS, Fig. 1 is made in terms of the percent change in CHL. There are relatively larger changes along the Liman Current and near the Tsugaru Strait. Although we can see the relative changes in CHL, we cannot see the long-term trend to project changes in CHL to the near future. The “trend” is defined as the overall tendency of the data over its entire time span, which will presumably continue into the future when new observations are added. Accordingly, the long-term trend is sensitive to the periods of measurement, despite the wide ranges of CHL changing. Fig. 2 shows the linear CHL trends, suggesting that the regional CHL trends are not the same but rather depend on geographic location. In general, the linear trends are high with an order of $[0.06 \text{ mg m}^{-3}] \text{ yr}^{-1}$ along the Liman Current from the Tartar Strait and to the west off the coast of the Tsugaru Strait and the Yamato Basin. In contrast, negative linear trends appear mainly in the southwest regions, especially along the EKWC (order of $[-0.03 \text{ mg m}^{-3}] \text{ yr}^{-1}$). Similar to the linear trends of CHL, the SST trends are also found (not shown). The SST linear trends reveal geographic unevenness and vary from $-0.1 \text{ }^\circ\text{C yr}^{-1}$ near the coast of the Korean Peninsula (especially approximately 40°N , 131°E) to $0.4 \text{ }^\circ\text{C yr}^{-1}$ near the west coast of Japan (especially 38°N , 136°E). According to Jo et al. [2014], the most significant warming appears in the long-term SST trends based on approximately 40 yr of SST measurements off the coast of the EJS, where it approaches $+0.05 \text{ }^\circ\text{C yr}^{-1}$.

In addition to direct comparisons between CHL and SST trends, we computed correlation coefficients between the monthly mean CHL and SST data for the last ten years (Fig. 2), showing negative correlation coefficients in most of the regions because the lower SST is aligned with higher CHL concentrations. Although linear trends enable us to easily understand how CHL and SST have changed over the observation period, it is not possible to understand non-linear processes in the CHL and SST signals over time.

As will be demonstrated, whereas non-linearity is dominant over linearity in CHL variability, linearity is dominant over non-linearity in SST variability within the EJS. Because of this scaling, we extracted non-linear signals from the CHL time series using the residuals of the EEMD. Fig. 3 was made to illustrate how to decompose the CHL time series and obtain non-linear trends from the residuals of the EEMD. As described in Fig. 3, the CHL time series was decomposed into five modes for different time scales, enabling us to understand at what time scales CHL is varying. Furthermore, the residuals of the EEMD show the adaptive data trends, or non-linear trends. As we stated earlier, this study aims to analyze the non-linear characteristics of CHL rather than merely interpret different scales of CHL variability. Because we can decompose CHL time series into oscillatory signals and a residual (or a trend) using EEMD (Fig. 3), we considered the EEMD residual the CHL trend, which is well-documented by Ezer and Corlett (2012). Most of the CHL trends derived from the EEMD residual were non-linear (Fig. 4).

Most of the applications for EEMD have been employed to analyze each mode with different frequencies. However, in this study, the focus is on the trend. The method is to separate oscillatory modes from the trend. The non-linear trend (residual of EEMD) is well examined based on long-term tide measurements along the Chesapeake Bay (Ezer and Corlett, 2012). This study demonstrates that the EEMD is robust within an acceptable statistical confidence level and that the trends are comparable with results obtained by other methods. The statistical confidence interval is calculated using a standard bootstrap method (Mudelsee, 2010).

To examine the geographically uneven trends and non-linear processes of CHL, we removed all oscillatory signals, such as the intra-annual, annual, and inter-annual modes from the monthly mean CHL data (shown in Fig. 3). Two specific cases are illustrated in Fig. 4: one is for a downward trend, and the other is for an upward trend. The linear CHL trend (blue line) shows a linearly increasing slope, but this does not represent the CHL variability (black line, decreasing after 2010). The non-linear trend (red line)

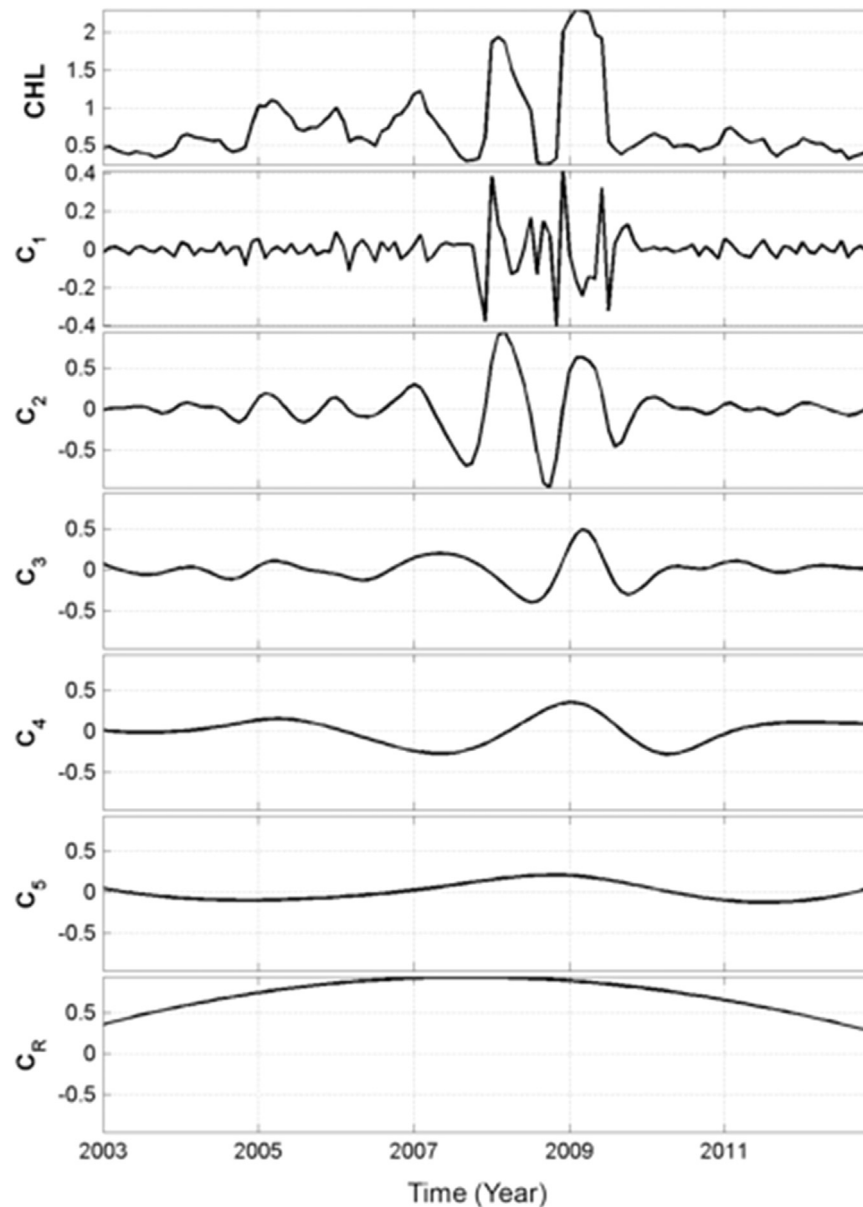


Fig. 3. Using EEMD, time series of CHL at one location (48°N, 141.5°E) was decomposed into five modes (C_1 to C_5) and a residual (C_R). The modes are intra-annual (C_1), annual (C_2), inter-annual (C_3 to C_5), respectively.

represents the actual CHL variability and has a turning point after approximately 2008, showing decreasing CHL in recent years. The opposite case is also shown in Fig. 4b. Whereas the linear trend is underestimated (blue line), especially for the years 2003 through 2005, the non-linear trend (red line) represents the overall CHL change over the time, and has an upward turning point circa 2008. As demonstrated in Fig. 4, we obtained non-linear trends for the EJS.

To examine the statistical confidence interval for the non-linear CHL trend derived from the EEMD residual, we used a standard bootstrap simulation (Mudelsee, 2010). The specific cases were conducted by Ezer and Corlett (2012) for their analysis. The main idea is to randomly resample the data many times to calculate errors and confidence intervals. As Fig. 5 shows, the simulated mean non-linear CHL through the bootstrap method (red line) is very close to the original CHL derived from EEMD residual (black line) and is within the 95% confidence level (red dot-line). Likewise, all non-linear CHL trends used in Figs. 6 and 8 were applied to CEOF and the timing of phase changes.

To understand the spatial and temporal variability in the non-linear trend of CHL, the CEOF was employed. With the CEOF modes, we analyzed the variability of the waters in the EJS and addressed the question of how CHL has changed over the past ten years with respect to spatial and temporal variability. It is worth noting that annual variability is the most significant signal when the monthly mean CHL data are applied to CEOF compared to any other frequencies. Thus, we removed all oscillatory signals using the EEMD and used only the residual signals as a non-linear time series of CHL. The advantage of using non-linear trend signals for the CEOF is that we can determine their spatial and temporal changes.

The CEOF shows the spatial features at different scales (Fig. 6). The first mode, with 95.6% of the variance, shows high variability near the Tartar Strait and the Tsugaru Strait, as well as low variability near the Ulleung Basin. The first temporal CEOF has a turning point in approximately 2007. From 2003 to 2007, CHL decreased over 4 yr, whereas from 2007 to 2012, CHL increased for 6 yr. In addition, the phase function (red dots) shows an eastward

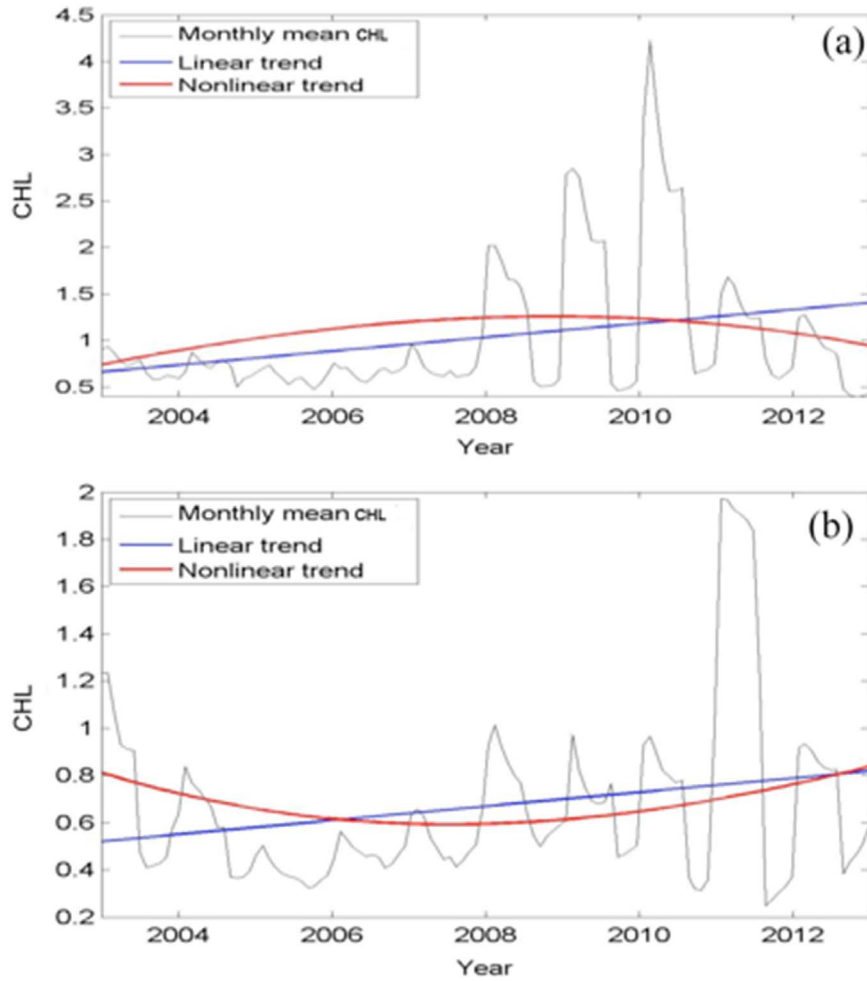


Fig. 4. Monthly mean CHL (black), linear trends, and non-linear trends derived from EEMD residuals of CHL at 48°N, 141.5°E (a) and 41°N, 130.8°E (b). Whereas the monthly mean CHL in (a) shows a downward slope after approximately 2008, that in (b) shows an upward slope after 2008.

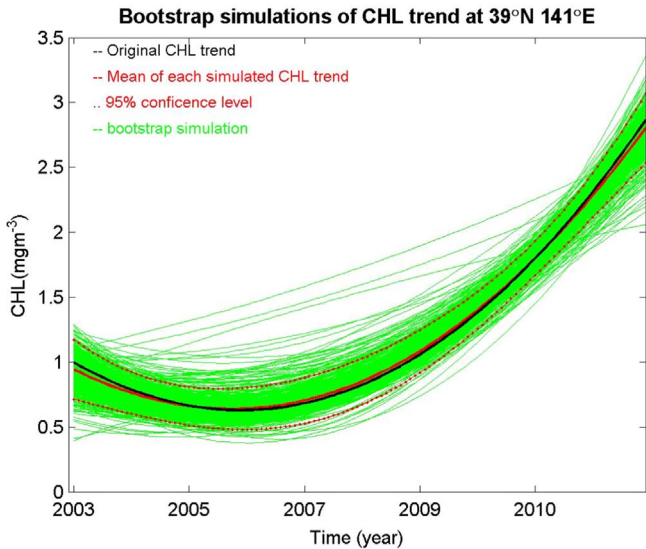


Fig. 5. Bootstrap simulations of the CHL non-linear trend to examine the significance level. It was simulated 100 times ($N=100$).

phase of 0.14π /month and a strong shift in approximately 2007.

The second mode, with 4.1% of the variance, mainly shows the negative and positive maxima at approximately 40°N 130°E and 40°N 140°E, respectively. The second temporal variability has a

downswing turning point in approximately 2009. From 2003 to 2009, CHL increased for 6 yr, whereas from 2009 to 2012, CHL decreased for 4 yr. Furthermore, the phase function (red dots) shows a westward phase of -0.08π month $^{-1}$, which is much slower than the first eastward CEOF.

The first two modes account for 99.7% and the corresponding errors in eigenvalues are very small when compared with the eigenvalues of each mode (Fig. 7). Whereas the first temporal mode suggests that the 95.6% of general CHL changes have the turning points circa 2007, the second temporal mode reveals that the CHL has a downturn trend in 2009. Although we can understand the general spatial and temporal changes from CEOF analysis, we may not be able to determine exactly when the specific regional changes occur. For instance, do all high or low spatial variances in modes 1 and 2 vary together over time? Or, if the trends change, how and when do they change? Due to the limited observations, these questions will be answered by examining the timing of the turning points, which indicate when the trend changes, either positively or negatively (Eq. (4)).

To examine the errors in the eigenvalues, we used the North's rule-of-thumb (North et al., 1982).

$$\delta\lambda_k \approx \lambda_k \sqrt{\frac{2}{N}} \quad (6)$$

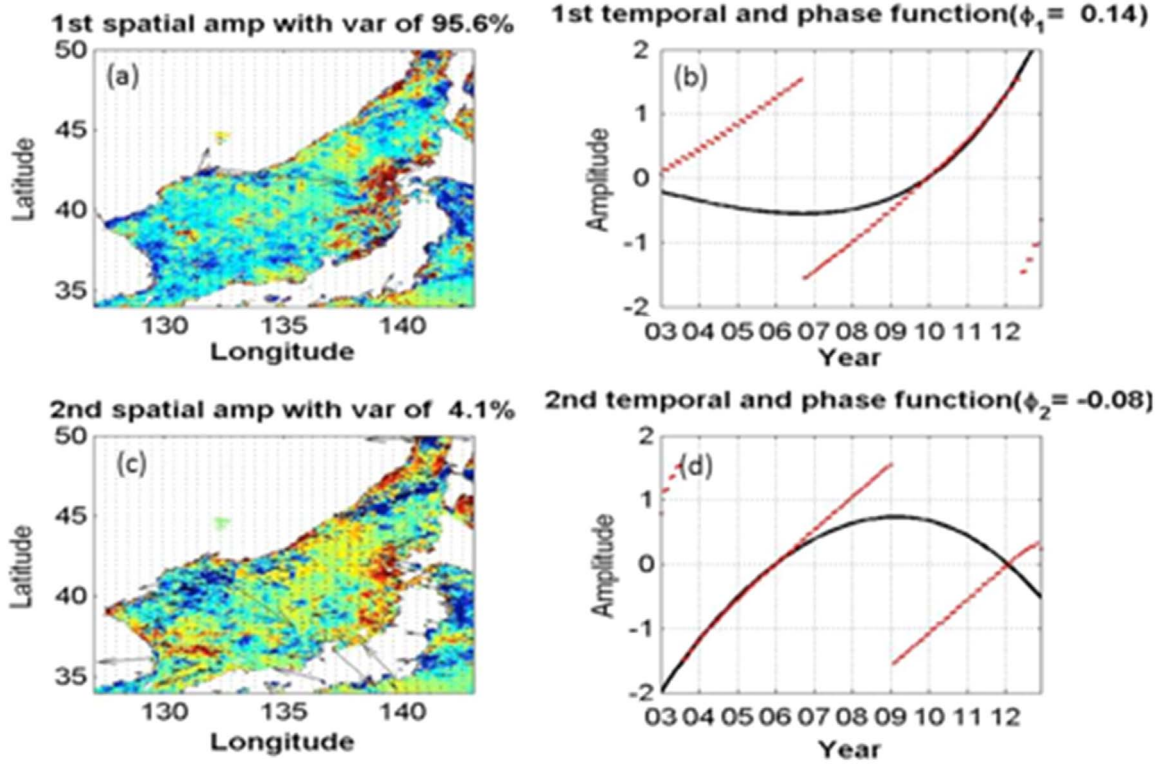


Fig. 6. The first two spatial CEOF (a and c) and temporal CEOF (b and d). The first and second modes account for 95.6% and 4.1%, respectively. The red dots in Fig. 5b and 5d represent the phase function.

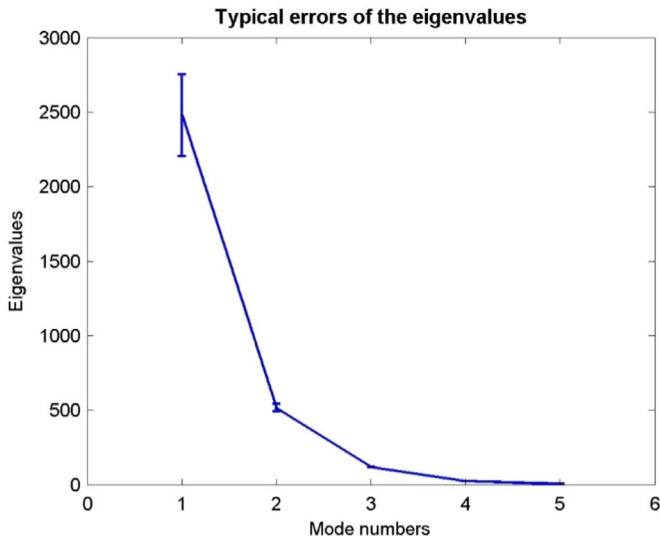


Fig. 7. Typical errors of the eigenvalues used in Fig. 6.

$$\delta e_k \approx \frac{\delta \lambda_k}{\lambda_j - \lambda_k} \cdot e_j \quad (7)$$

where λ_k is the eigenvalue closest to λ_j and N is the number of measurements. δe_k is the typical error in eigenvalues. Accordingly, δe_k is the previous error in eigenvalues in the process in Eq. (7). The specific processes is well documented in North et al. (1982) and Sparnocchia et al. (2003). One can see the small error bars for the eigenvalues for each mode.

3.2. Determination of the timing of phase changes in CHL

How can we determine local regime shifts with limited

observations? It is nearly impossible without long enough series of observations. However, we can determine sudden phase changes in CHL in a similar way as we study a regime shifts using the Cumulative Sums. Accordingly, the turning points for non-linear trends can indeed be used to determine the timing of phase changes in CHL, the main objective of this study. A turning point is defined as a local minimum or maximum in the non-linear trend. Although we cannot determine turning points from linear trends, we are able to determine them from the non-linear trends. The use of EEMD residuals as a non-linear trend has been discussed (e.g., Ezer and Corlett, 2012). The non-linear trend contains either a local maximum or minimum or a linear relation. The strength of the residual lies in its ability to virtually eliminate the problem of contamination from interannual, decadal and multi-decadal variability.

The timing of turning points was determined (Fig. 8). Based on these processes, we determined either a local maximum showing a downward trend or a local minimum showing an upward trend. In other words, we examined how CHL trends changed during an increase in the rate of CHL, eventually becoming a decrease, and vice versa. Whereas Fig. 8a shows a downswing in the rate of CHL that turns into another downswing, Fig. 8b shows an upswing in the rate of CHL that turns into another upswing. The color scale indicates the specific time when the turning points occur in the different regions. The masked white areas in the EJS do not have any non-linear trends (neither local maxima nor minima in the EEMD residual) so no turning points exist, implying that the locations for the non-linear trends dominate those of the linear trends. The ratio between regions with non-linear and regions with linear CHL trends is 9:1.

Areas I, II and III in Fig. 8a have turning points occurring approximately in the years 2007, 2009, and 2008, respectively. The downward turning features are comparable with the second spatial CEOF (Fig. 6c). Thus, there are two years of time differences between upward and downward turning trends in the CEOF,

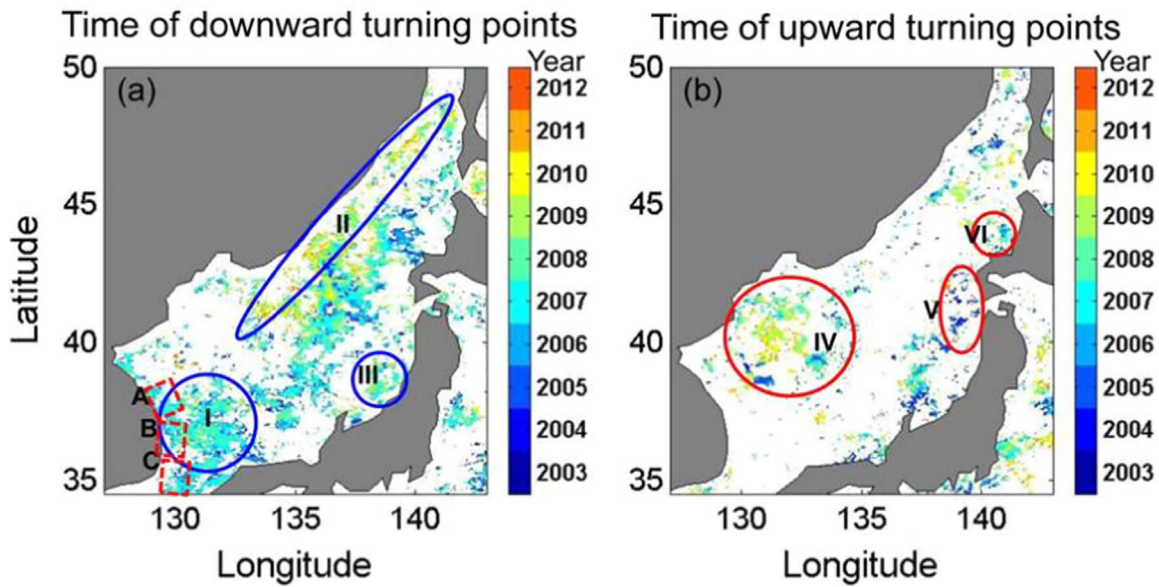


Fig. 8. Timing of downward turning points (a) and upward turning points (b) determined from the residuals of CHL (as shown with Fig. 4). Provinces A to C were used to compare fish changes (Fig. 9) with the timing of turning points. The red boxes off Provinces A, B, and C represent the total fish catch data collected.

suggesting that some time is needed to adjust CHL phases from one phase to another. (Fig. 6d). Similarly, Areas IV to VI in Fig. 8b have turning points approximately in the years of 2010, 2005 and 2007, respectively. The upswing turning features are comparable with the first spatial CEOF (Fig. 6a). Thus, there are six years of time differences in the CEOF (Fig. 6b).

An intriguing question is what type of force controls the local regime shift. In Fig. 8, the timing of downward or upward turning points mainly occurs approximately in 2007 (shown with green) or in 2010 (shown with yellow). We examined these timings with the MEI index (Fig. 9). The ENSO events also have an impact on CHL in the EJS, as discussed in the introduction. While small and large El Niño events occur in 2003–2006, 2007, 2010 and 2012, the

La Niña events occur in 2008–2009, 2011. Because we are examining sudden changes in CHL, the Cumulative Sums was applied to the MEI index, as shown with a red curve in Fig. 9. Local maxima were found in the years of 2007 and 2010, followed by the years 2005–2006. The year 2007 was the timing of a downward turning point, and most of the regions in Fig. 8a are relevant (especially Areas I and III). Similarly, the year 2010 was the timing of a downward turning point in Area II in Fig. 8a. The influence of the local maxima in the years 2005–2006 appears to be very small in Fig. 8a. The influence might be weakened due to the following event in the year 2007.

As introduced in the introduction, research shows that the relations between ENSO events and CHL change. However, they also

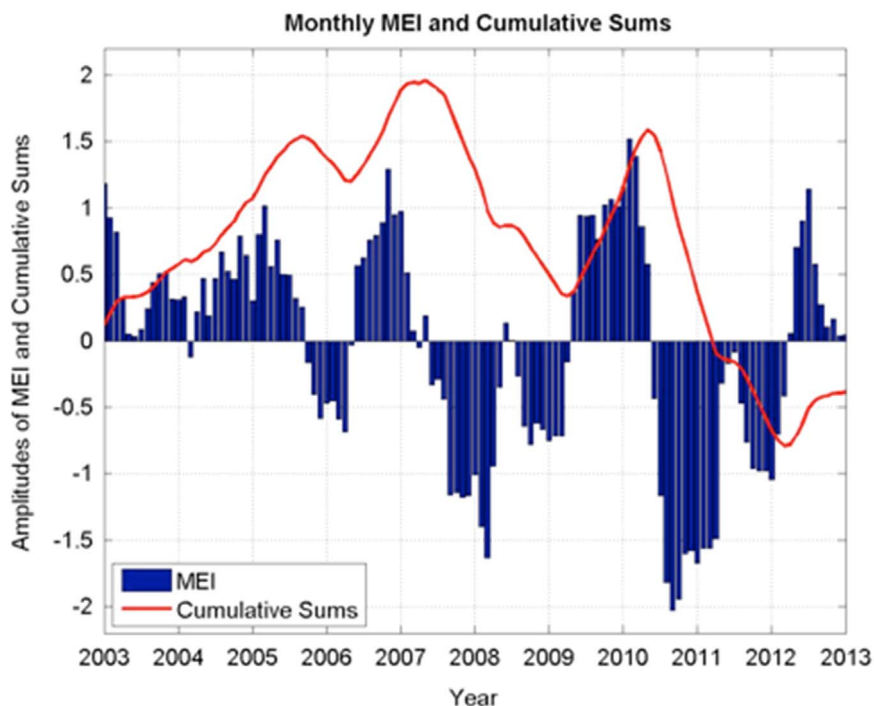


Fig. 9. Monthly mean Multivariate ENSO index (MEI) (red line) and Cumulative Sums from January 2003 to December 2012. (For interpretation of the references to color in this figure legend, the reader is referred to the web version of this article.)

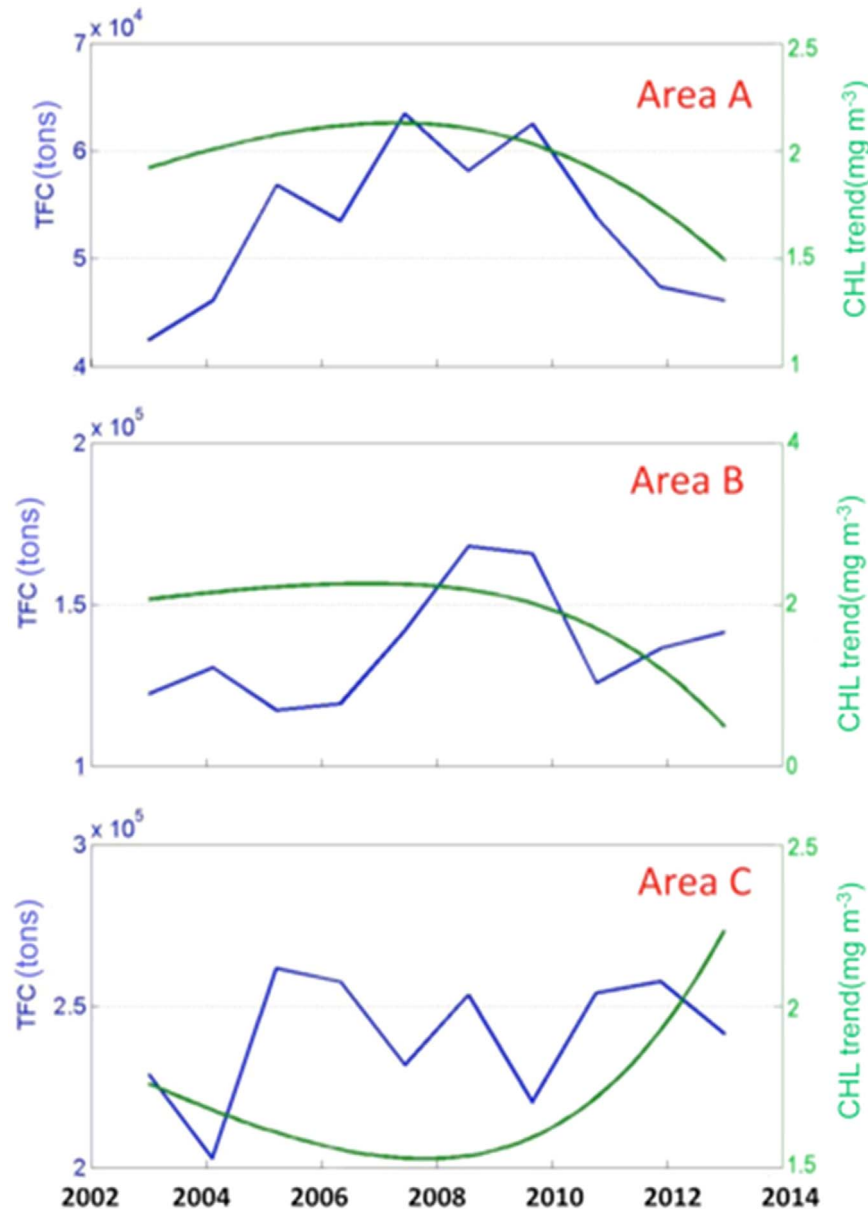


Fig. 10. Total fish catches per year (TFC) shown with blue lines and non-linear CHL trend near the east coast of the EJS. Different areas are shown in Fig. 8a: off the coasts of Areas A (37–38°N, 128–129°E) (a), B (35.4–37°N, 128–129.5°E) (b) and C (34.5–35°N, 128.5–129°E) (c) represent the provinces of Gangwon-do, Gyeongsangbuk-do, and Busan, respectively. To illustrate the fish data and CHL in all three regions, the CHL was multiplied by 2 for Areas A and B. (For interpretation of the references to color in this figure legend, the reader is referred to the web version of this article.)

demonstrate the difficulties of estimating the relations specifically because many signals are merged in both measurements. Thus, in this study we used Cumulative Sums to detect the timing of phases when MEI changed significantly, which was compared with that timing of CHL upward or downward trends.

The upward turning points in Fig. 8b occurred in the years 2010, 2005, and 2007 for Areas IV, V and VI, respectively. It is worth noting that we only could find some relationship between local maxima from Cumulative Sums and both the timing of downward and upward turning points. It seems that the local minima in the years of 2009 and 2010 from Cumulative Sums are too short to be dominant because of the local maxima in the year 2010.

3.3. Impact of CHL phase changes on total fisheries catch

What does the timing of the downswing and upswing turning

points of CHL mean for fishery abundance? We used the catch data from Korean marine capture fisheries at three different locations to interpret these turning points. The locations are provinces A and B and city C, Busan. Each location is indicated in Fig. 8a. Province A is directly under the influence of the North Korean Cold Water originating from the Liman Current. Province B is under the influence of the EKWC, and city C is located near the Korean Strait. In Fig. 10, the blue and green lines represent the annual total fish catch (TFC) and non-linear trend of CHL at three locations, respectively. We determined the timing of the turning points. Whereas provinces A and B have a downward turning point in CHL in 2007–2008, Busan has an upward turning point in CHL in 2008 over 10 yr. The annual total fish catch off the coast of Areas A to C varies from a minimum of 4.2×10^4 t in 2003, 1.2×10^5 t in 2003, and 2.3×10^5 t in 2004 to a maximum of 6.25×10^4 t in 2007, 1.7×10^5 t in 2008, and 2.6×10^5 t in 2005, respectively. One can see that the local maxima and minima of the TFC are comparable

to the timing of the turning points of CHL in Fig. 10, implying that the TFC changes are similar to the CHL non-linear trends.

Because there are no long-term CHL measurements to resolve climatic regime shifts, we focus on CHL phase changes, which are influenced by significant changes from the North Pacific. As climatic regime shift affects annual variability in the catches of major fisheries (Zhang et al., 2007), the timing of phase changes in CHL also affects the annual TFC off the coast of Korea. Accordingly, Fig. 10 suggests that the trends of downward turning and upward turning points in other regions (Fig. 8) may have similar TFC trends as illustrated with Fig. 10. Specifically, while the Areas I, II and III in Fig. 8a have downward TFC trends approximately 2007, 2007 and 2010, respectively as Areas A and B have (Fig. 10). Similarly, the Areas IV, V, and VI, in Fig. 8b have upward TFC trends in approximately 2009, 2005 and 2006, respectively, as has Area C (Fig. 10).

It is worth noting that the TFC data do not represent any specific fish species. The TFC include any fish caught near the Areas A, B, and C. Furthermore, although we used the TFC data for the specific provinces and a city, some of fish could be caught other near regions. However, with some uncertainties we tried to examine the relationship between long-term non-linear CHL trends and the trend of TFC. Because it is not possible to show how the specific fish species are related to the non-linear trends of CHL due to limited fish sampling data, we leave it for our future work.

4. Summary

The CHL time series has either linear or non-linear trends, which depend on the geographic locations (Fig. 2). In addition to discussing the linear trend of CHL in the EJS, we analyzed non-linear processes in the CHL observations. To understand non-linear processes in the observations, we decomposed CHL into empirical modes using EEMD and determined the timing of turning points derived from the residual of the decomposed CHL. The non-linear trends can be separated into the categories of either an upward trend or downward trend (Figs. 4 and 8). The linear trends in Fig. 2 shows similar spatial features in the first spatial CEOF, which has an upswing turning point in the first temporal CEOF (Fig. 6b) and the turning points highlighted in areas IV, V, and VI (Fig. 8b). Similarly, the linear trends in Fig. 2 show some of the spatial features of the second spatial CEOF, which has a downswing turning point in the second temporal CEOF (Fig. 6d), as well as the highlighted turning points in areas I, II, and III (Fig. 8a). Thus, despite the limited fishery catch data, we were able to identify the change in fish catches that are closely related to the non-linear CHL trends (Fig. 10).

Our findings can be summarized as follows.

1. The linear CHL trend varies from -0.06 to 0.1 [mg m^{-3}] yr^{-1} , depending on the geographic location. The relatively high CHL has relatively high positive correlations with the non-linear SST trend (not shown).
2. Whereas the first CEOF (Fig. 6a and 6b) is related to upswing turning points (Fig. 8b), the second CEOF (Fig. 6c and 6d) is related to downswing turning points in the non-linear trends (Fig. 8a). Additionally, whereas the spatial CEOF represents the general phase and amplitude changes, the timing of the turning points determined from non-linear trends shows the specific time during which the changes occurred.
3. Whereas the downward turning points occurred approximately in 2004–2007 around the Ulleung Basin and the west coast of Japan, the upward turning points occurred approximately in 2010 in the middle of the west EJS and in 2008 in the northeast of the EJS.

4. The timing of phase changes in CHL occurred in the year 2007, explained by the Cumulative Sum of MEI (Figs. 6 and 9).
5. The local regime shifts determined from the non-linear CHL trends agree very well with the TFC, as illustrated by the coasts of the two provinces, Gangwon-do (Area A) and Gyung-sang-book-do (Area B), and the city of Busan (Area C) (Fig. 10).

We also examined whether the results based on the OC3 algorithm are different from those based on the Chlor-a algorithm based on an empirical relationship derived from in situ measurements of chlorophyll concentration and blue-to-green band ratios of in situ remote sensing reflectances (Rrs) (http://oceancolor.gsfc.nasa.gov/cms/chlor_a). Because we could not find significant differences between the two algorithms, we concluded that the analysis based on two different algorithms for CHL is the same in the EJS. Although there are some biases between the two algorithms, our analysis is still valid. Because our study focuses on determining the timing of turning points based on the non-linear trend of CHL, the beginning and the last CHL data points are not very significant to determining turning points.

The continuous CHL observations can be used to understand changes in fishery resources in time and space in response to local phase changes in CHL resulting from climate change events. However, it is not clear whether changes in the TFC are primarily a response to the ENSO events unless we use a numerical model to examine each case for different physical forces, such as winds, currents, and heat flux.

Acknowledgments

This research was supported by the Korea Polar Research Institute (KOPRI: PG15010) and Korea Institute of Science and Technology Information (KISTI), and was partly supported by the project of “Long-term change of structure and function in marine ecosystems of Korea”, funded by the Ministry of Oceans and Fisheries, Korean. NASA Goddard Space Flight Center, Ocean Ecology Laboratory, Ocean Biology Processing Group. Moderate-resolution Imaging Spectroradiometer (MODIS) Aqua Ocean Color Data; 2014 Reprocessing. NASA OB.DAAC, Greenbelt, MD, USA. http://dx.doi.org/10.5067/AQUA/MODIS_OC.2014.0.

References

- Bertolo, A., Lacroix, G., Lescher-Moutouf, F., Sala, S., 1999. Effects of physical refuges on fish-plankton interactions. *Freshw. Biol.* 41, 795–808.
- Breaker, L.C., 2007. A closer look at regime shifts based on coastal observations along the eastern boundary of the North Pacific. *Cont. Shelf Res.* 27, 2250–2277.
- Ezer, T., Corlett, W.B., 2012. Is sea level rise accelerating in the Chesapeake Bay? A demonstration of a novel new approach for analyzing sea level data. *Geophys. Res. Lett.* 39, L19605. <http://dx.doi.org/10.1029/2012GL053435>.
- Hawkins, D.M., Howell, D.H., 1998. *Cumulative Sum Charts and Charting for Quality Improvement*. Springer, New York.
- Huang, N.E., Shen, Z., Long, S., Wu, M., Shih, H., Zheng, Q., Yen, N.C., Tung, C., Liu, H., 1998. The empirical mode decomposition and Hilbert spectrum for non-linear and nonstationary time series analysis. *Proc. R. Soc. Math. Phys. Eng. Sci.* 454, 903–995.
- Huang, N.E., Wu, Z., 2008. A Review in Hilbert-Huang Transform: Method and Its Applications to Geophysical Studies. *Rev. Geophys.* 46, RG2006. <http://dx.doi.org/10.1029/2007RG000228>.
- Jo, Y.-H., Breaker, L.C., Tseng, Y., Yeh, S.-W., 2014. A temporal multiscale analysis of the waters off the east coast of South Korea over the past four decades. *Terr. Atmos. Ocean. Sci.* 25, 415–434. <http://dx.doi.org/10.3319/TAO.2013.12.31.01> (Oc).
- Kim, H.C., Yoo, S., Oh, I.S., 2007. Relationship between phytoplankton bloom and wind stress in the sub-polar frontal area of the Japan/East Sea. *J. Mar. Syst.* 67, 205–216.
- Kim, Yoo, 1996. Did Climate Regime Shift in 1976 in the North Pacific Occur in Korean Waters? *Ocean Policy Res.* 11 (1), 133–149.
- Kim, S., Kang, S., 2000. Ecological variations and El Niño effects off the southern coast of the Korean Peninsula during the last three decades. *Fish. Oceanogr.* 9

- (3), 239–247.
- Merrifield, M.A., Guza, R.T., 1990. Detecting propagating signals with complex empirical orthogonal functions: a cautionary note. *J. Phys. Oceanogr.* 20, 1628–1633. [http://dx.doi.org/10.1175/1520-0485\(1990\)020<1628:DPSWCE>2.0.CO;2](http://dx.doi.org/10.1175/1520-0485(1990)020<1628:DPSWCE>2.0.CO;2).
- Page, E.S., 1954. Continuous inspection schemes. *Biometrika* 41, 100–115.
- Mudelsee, M., 2010. *Climate Time Series Analysis: Classical Statistical and Bootstrap Methods*. Springer, Dordrecht, Netherlands, p. 474.
- North, G., Bell, T.L., Cahalan, R.F., Moeng, F., 1982. Sampling errors in the estimation of empirical orthogonal functions. *Mon. Weather Rev.* 110, 699–706.
- Platt, T., Fuentes-Yaco, C., Frank, K.T., 2003. Marine ecology: spring algal bloom and larval fish survival. *Nature* 423, 398–399. <http://dx.doi.org/10.1038/423398b>.
- Polovina, J.J., Howell, E., Kobayashi, D.R., Seki, M.P., 2001. The transition zone chlorophyll front, a dynamic global feature defining migration and forage habitat for marine resources. *Prog. Oceanogr.* 49, 469–483.
- Seung, Y.H., Kim, K., 1989. On the possible role of local thermal forcing on the Japan Sea circulation. *J. Korean Oceanogr. Soc.* 24, 29–38.
- Son, S., Campbell, J., Dowell, M., Yoo, S., 2005. Decadal variability in the Yellow and East China Seas as revealed by satellite ocean color data (1979–2003). *Indian J. Mar. Sci.* 34 (4), 418–429.
- Sparnocchia, S., Pinardi, N., Demirov, E., 2003. Multivariate empirical orthogonal function analysis of the upper thermocline structure of the Mediterranean Sea from observations and model simulations. *Ann. Geophys.* 21, 167–187.
- Tian, Y., Nashida, K., Sakaji, H., 2013. Synchrony in the abundance trend of spear squid *Loligo bleekeri* in the Japan Sea and the Pacific Ocean with special reference to the latitudinal differences in response to the climate regime shift. *ICES J. Mar. Sci.* . <http://dx.doi.org/10.1093/icesjms/fst015>
- Von Storch, H., Zwiers, F.W., 1999. *Statistical Analysis in Climate Research*. Cambridge University Press.
- Wetherill, G.B., Brown, D.W., 1991. *Statistical Process Control, Theory and Practice*. Chapman & Hall, London.
- Wu, Z., Huang, N.E., 2009. Ensemble empirical mode decomposition: a noise-assisted data analysis method. *Adv. Adapt. Data Anal.* 1, 1–41.
- Wu, Z., Huang, N.E., 2005. Statistical significance test of intrinsic mode functions. In: Huang, N.E., Shen, S.S.P. (Eds.), *Interdisciplinary Mathematical Sciences vol. 5*; 2005, 311 p. (Chapter 5).
- Yamada, K., Ishizaka, J., Yoo, S., Kim, H.C., Chiba, S., 2004. Seasonal and interannual variability of sea surface chlorophyll a concentration in the Japan/East Sea (JES). *Prog. Oceanogr.* 61, 193–211.
- Yoo, S., Kim, H.C., 2004. Suppression and enhancement of the spring bloom in the southwest East Sea/Japan Sea. *Deep Sea Res.* 51, 1093–1111.
- Zhang, C.I., Yoon, S.C., Lee, J.B., 2007. Effects of the 1988/89 climatic regime shift on the structure and function of the southernwestern Japan/East Sea ecosystem. *J. Mar. Syst.* 67, 225–235.
- Zhang, C.I., Lee, J.B., Seo, Y.I., Yoon, S.C., Kim, S., 2004. Variations in the abundance of fisheries resources and ecosystem structure in the Japan/East Sea. *Prog. Oceanogr.* 61, 245–265.
- Zhang, C.I., Lee, J.B., Kim, S., Oh, J.H., 2000. Climatic regime shifts and their impacts on marine ecosystem and fisheries resources in Korean waters. *Prog. Oceanogr.* 47, 171–190.